Axial apodization in 4Pi-confocal microscopy by annular binary filters

Manuel Martínez-Corral and Amparo Pons

Departamento de Óptica, Universidad de Valencia, 46100 Burjassot, Spain

María-Teresa Caballero

Departamento de Óptica, Universidad de Alicante, P.O. Box 99, 03080 Alicante, Spain

Received September 18, 2001; revised manuscript received March 8, 2002; accepted March 12, 2002

We present a novel technique for considerably decreasing the sidelobe height of the axial point-spread function of one-photon 4Pi-confocal microscopes. By means of a numerical example, in which the ratio between the excitation and the fluorescence wavelengths was set to $\epsilon = \lambda_{exc}/\lambda_{det} = 0.8$, we show that simply inserting a pair of properly designed two-ring binary masks in the illumination set allows the height of the axial sidelobes to be reduced from 20% to 5% of the height of the central peak. This allows one to receive the full benefit of the strong narrowness of the central lobe provided by the 4Pi-confocal technique. © 2002 Optical Society of America

OCIS codes: 220.1230, 200.1230, 180.1790, 100.6640.

1. INTRODUCTION

One of the main limitations of optical microscopy is the diffraction limited resolution, which is determined by the wavelength of the light and the numerical aperture (NA) of the lenses.[1] This limitation is more evident in biological imaging, which deals with transparent three-dimensional objects. In this case not only the lateral resolution but also the axial resolution is important. However, even when dealing with confocal microscopy, which is a technique whose main feature is its axial discrimination,[2] the axial resolution is approximately three times poorer than its lateral counterpart.

4Pi-confocal microscopy is a recently developed imaging technique specifically designed to achieve high resolution in the axial direction.[3,4] To this end, in the 4Pi-confocal microscope two opposing high-NA objectives are used for coherently illuminating and/or detecting the same point of a fluorescent sample. Then two spherical wave fronts interfere in the common focus so that the total aperture is doubled. The interference process yields an intensity point-spread function (PSF) with a main axial maximum that is approximately four times narrower than the one corresponding to a confocal microscope. However, the mere narrowing of the central lobe is insufficient for improving the axial resolution. Note that (as in a Young experiment) the resulting axial PSF can be expressed as the product between a $\cos^2$ factor (the interference factor), whose period is proportional to the wavelength, and a sinc^2 factor (the diffraction factor), whose width is proportional to the inverse of the lenses' NA. Then, the higher the value of NA, the smaller the axial sidelobes. However, even for the largest value of the NA, the axial PSF exhibits sidelobes that are too high. These secondary maxima reduce the benefit of narrowing the central peak because they can lead to ambiguity in the image.

To overcome this problem the use of two-photon excitation[4–6] and deconvolution[7–9] techniques have been proposed. With two-photon excitation the contribution of secondary maxima of the illumination PSF is reduced because of the squared dependence of the excitation on the illumination intensity. However, the ability of two-photon excitation as a sidelobe-reducing tool in 4Pi-confocal microscopy proceeds mainly from the considerable difference between the excitation wavelength and the fluorescence wavelength. Owing to such difference, the illumination and the detection PSFs have quite different scales such that the secondary peak of the illumination PSF is multiplied by low values of the detection PSF, and, in addition, the secondary peak of the detection PSF is multiplied by low values of the illumination PSF. This multiplicative process yields a significant reduction of the secondary axial lobes of the 4Pi PSF.

In this paper we propose an alternative technique for reduction of the axial sidelobes. The technique is based on the use of pupil filters in the illumination set of a 4Pi-confocal microscope. The design of pupil filters to overcome the limits in resolution imposed by diffraction in imaging systems is a mature science.[10–12] The main drawback of using pupil filters in conventional imaging systems is that the narrowness of the central lobe of the intensity PSF is obtained at the expense of higher sidelobes, which compromises the real gain in resolution. However, if a confocal-scanning architecture is used, this collateral effect is overcome. In this sense, during the past few years the use of pupil filters has been proposed to improve the lateral,[13–15] the axial,[16] and the three-dimensional[17–22] resolution of confocal-scanning micro-

0740-3232/2002/081532-05$15.00

scopes. As far as we know, the only attempt to use pupil filters in 4Pi-confocal microscopy was reported in Ref. 23, where the use of annular apertures produced a slight narrowing in the lateral PSF but an enlargement of axial sidelobes.

What we propose in this paper is the use of annular binary masks in one-photon 4Pi-confocal microscopy to reduce the strength of the PSF axial sidelobes. The cornerstone of our method is to produce on the PSF an effect similar, in some way, to the one produced by two-photon excitation. Therefore we need to design pupil filters with the ability to compress the illumination axial PSF so that in the confocal-multiplicative process the secondary peak of the illumination axial PSF is multiplied by low values of the detection axial PSF, and vice versa. In other words, we propose the use of axially superresolving pupil filters, which in conventional imaging produce high axial sidelobes, to paradoxically obtain an apodization effect[24] in 4Pi-confocal microscopy, i.e., a severe reduction of the strength of axial sidelobes.

2. BASIC THEORY

To calculate the axial intensity PSF of a 4Pi-confocal microscope, we start by considering the electric field in the focal region of an aberration-free lens illuminated by a linearly polarized wave front[5,25–27]; i.e.,

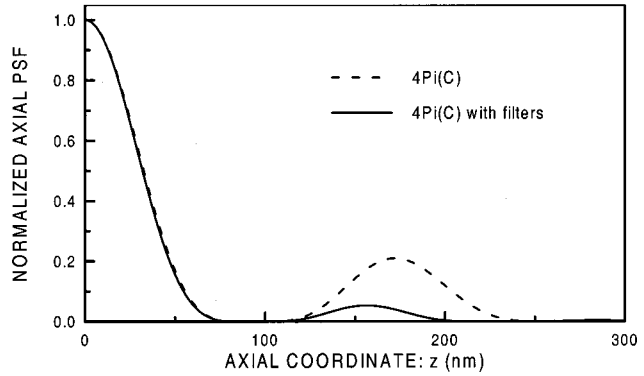

Fig. 1. Numerically evaluated axial intensity PSF for a 4Pi(C)-confocal microscope. The parameters for the calculation were $\lambda_{exc} = 350$ nm, $\epsilon = 0.8$, NA = 1.4

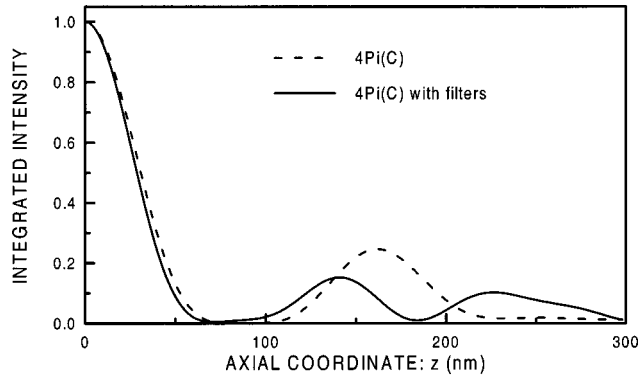

Fig. 2. Normalized z response to an infinitely thin fluorescent layer for a 4Pi(C)-confocal microscope. The parameters for the calculation are the same as in Fig. 1.

$$\mathbf{E}(u, v, \phi) = [I_0(u, v) + I_2(u, v)\cos 2\phi]\mathbf{i} + I_2(u, v)\sin 2\phi\mathbf{j} - 2iI_1(u, v)\cos\phi\mathbf{k}. \quad (1)$$

In Eq. (1), $I_n(u, v)$, with $n = 0,1,2$, are integrals over the lens aperture, and $u = 4nkz\sin^2\alpha/2$ and $v = nkr\sin\alpha$ are, respectively, the axial and the lateral focal coordinates expressed in optical units, α being the semiaperture angle. Finally, ϕ stands for the angle between the polarization direction of the incident field and the observation meridian plane.

Three different geometries for a 4Pi-confocal microscope have been proposed.[3] We concentrate our study on the so-called type-C geometry (the one that provides the highest axial resolution), in which by use of two opposing high-NA objectives the fluorescent sample is coherently illuminated and observed. In this case the PSF is given by

$$H(u, v, \phi) = |\mathbf{E}_{exc}(u, v, \phi) + \mathbf{E}_{exc}(-u, v, \phi)|^2 \times |\mathbf{E}_{det}(\epsilon u, \epsilon v) + \mathbf{E}_{det}(-\epsilon u, \epsilon v)|^2, \quad (2)$$

where random polarization of fluorescent light is assumed. In Eq. (2), the parameter $\epsilon = \lambda_{exc}/\lambda_{det}$ represents the ratio between the excitation wavelength and the fluorescence wavelength.

Since we are interested mainly in the analysis and engineering of the PSF along the optical axis we set $v = 0$ in Eq. (1) and find that $I_1(u, v = 0) = I_2(u, v = 0) = 0$. Then the axial PSF of the 4Pi(C)-confocal microscope, $H(u,0)$, depends only on the value of $I_0(u, v = 0)$.

As an example of the axial performance of these systems, in Figs. 1 and 2 we have depicted with the dashed curve the axial PSF and the z response of an infinitely thin fluorescent layer, respectively. The parameters for the numerical evaluation were $\lambda_{exc} = 350$ nm, $\epsilon = 0.8$, $n = 1.518$, and $\alpha = 67.5°$ (NA = 1.4). Note that although in both curves a narrow central peak is obtained, the axial sidelobes are too high.

3. DESIGN OF ANNULAR FILTERS FOR REDUCTION OF AXIAL SIDELOBES

As described in Section 1, our aim here is to design a pupil filter with the ability to compress at will the axial PSF of the illumination set of a 4Pi-confocal microscope. In other words, we need a pupil filter designed to obtain axial superresolution. The easiest solution to this task is the one reported in Ref. 16. The filters presented in that paper, which were designed to be used in the paraxial regime, are composed of two equal-area transparent annuli. However, 4Pi-confocal microscopes are useful only with high-NA objectives. Thus the procedure for designing axially superresolving pupil filters[16] should be reformulated by taking into account the high-NA regime. Note that, although in a 4Pi-confocal system the calculation of PSFs must be performed according to the vector theory, for the sake of making a comprehensive and simple design procedure we prefer to minimize the number of free parameters and develop the procedure in terms of the sca-

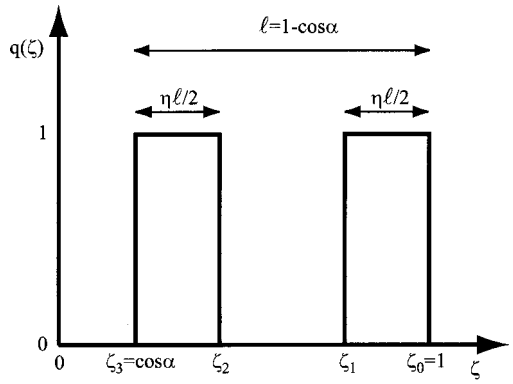

Fig. 3. Mapped amplitude transmittance, $q(\zeta)$, of an axially superresolving two-ring filter. The relation between the parameter ζ and the normalized radial coordinate in the filter plane is $r = (1 - \zeta^2)^{1/2}/\sin\alpha$. Then the actual normalized radii for the transparent annuli are $r_0 = 0$ and $r_1 = [1 - (1 - \eta l/2)^2]^{1/2}/\sin\alpha$ (inner annulus) and $r_2 = [1 - (\cos\alpha + \eta l/2)^2]^{1/2}/\sin\alpha$ and $r_3 = 1$ (outer annulus). The light efficiency of the filter is given by $\eta = r_3^2 - r_2^2 + r_1^2 - r_0^2$.

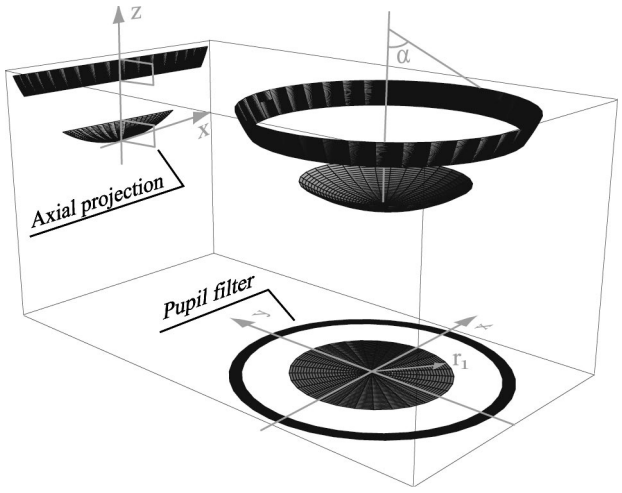

Fig. 4. Binary two-ring pupil filter whose axial projection consists of two equal-width rectangles. The shaded areas correspond to regions of transmittance equal to 1.

lar theory. To this end we consider the axial amplitude distribution provided by a focused scalar spherical wave[27]; that is,

$$h(u) = \int_0^{\alpha} A(\theta)\exp\left(i\,\frac{\cos\theta}{4\sin^2\alpha/2}u\right)\sin\theta\,\mathrm{d}\theta, \qquad (3)$$

where $A(\theta)$ is the apodization function and α the semiaperture angle. Note that apart from a factor $(1 + \cos\theta)$ within the integral, the function $h(u)$ is equivalent to $I_0(u, v = 0)$. After performing the nonlinear mapping

$$\zeta = \cos\theta, \qquad q(\zeta) = A(\theta), \qquad (4)$$

we can rewrite Eq. (3) as

$$h(u) = \int_{\cos\alpha}^{1} q(\zeta)\exp\left(i\,\frac{\zeta}{4\sin^2\alpha/2}u\right)\mathrm{d}\zeta. \qquad (5)$$

From the above equation it follows that the axial amplitude distribution in the focal region is governed mainly by the one-dimensional Fourier transform of the mapped apodization function $q(\zeta)$. Therefore, to obtain an axially superresolving effect equivalent to that reported in Ref. 16, it is necessary an apodization function $A(\theta)$ such that the mapped function $q(\zeta)$ consists of two equal-width rectangles (see Fig. 3).

The above reasoning can also be understood in terms of the Ewald sphere.[28,29] The amplitude transmittance of the two-ring binary mask is such that its axial projection consists of two equal-width rectangles; see Fig. 4. From this figure [and also from Eqs. (4) and (5)] it is apparent that the actual form of the binary filter depends on the width of both the rectangles and the semiaperture angle α.

4. NUMERICAL EXPERIMENT

We start this section by emphasizing that although the filter-design procedure has been developed on the basis of the scalar diffraction theory, in all our numerical evaluations we will use the vector equations and consider that the illumination wave fronts are linearly polarized. Then for calculating the axial PSF we use the equation that results from particularizing Eq. (1) to points in the optical axis ($v = 0$); that is,

$$\begin{aligned} E(u, v = 0) &= I_0(u, v = 0) \\ &= \int_0^{\alpha}(1 + \cos\theta)A(\theta) \\ &\quad \times \exp\left(i\,\frac{\cos\theta}{4\sin^2\alpha/2}u\right)\sin\theta\,\mathrm{d}\theta \\ &= \int_{\cos\alpha}^{1}(1 + \zeta)q(\zeta)\exp\left(i\,\frac{\zeta}{4\sin^2\alpha/2}u\right)\mathrm{d}\zeta. \end{aligned} \qquad (6)$$

To demonstrate the power of our approach, we performed a numerical experiment in which we inserted two copies of the same annular filter in both arms of the illumination set, as shown in Fig. 5. In this scheme relay lenses are used to focus the filters into the back focal plane of the objectives. Since the PSF-sidelobe-reduction

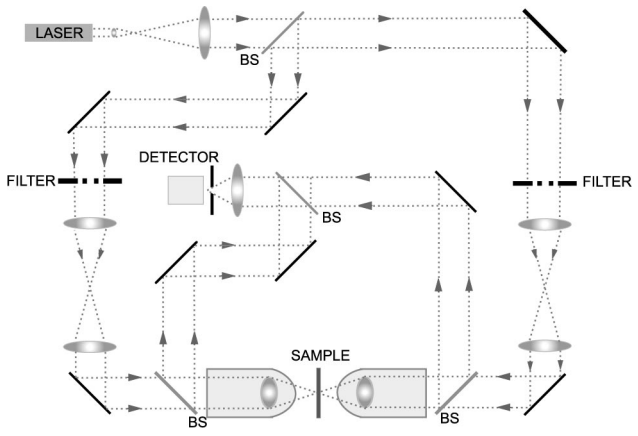

Fig. 5. Schematic geometry of a 4Pi(C) apodized confocal-scanning optical microscope. Relay lenses are used to focus the filters into the back focal plane of the objectives. BS, beam splitter.

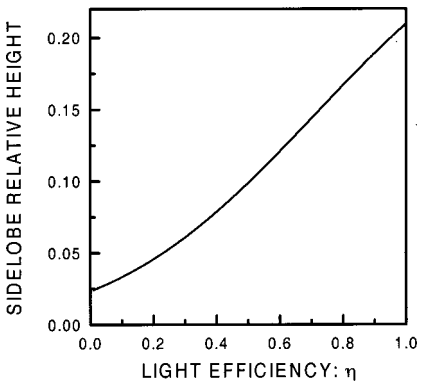

Fig. 6. Relative height of the axial sidelobe versus the light efficiency of the pupil filters.

capacity of the filters depends on the width of the rectangles, i.e., on the light efficiency of the filters η (see Fig. 3 caption for a comprehensive definition of parameter η), in Fig. 6 we have calculated the relation between η and the relative height of the axial sidelobe. The parameters used for the calculation were $\lambda_{exc} = 350$ nm, $\epsilon = 0.8$, NA = 1.4. From this figure it follows that the relation is almost linear except in the lower part of the curve, where the slope is smaller. Then, to optimize simultaneously the light efficiency of the filter and the sidelobe-reduction power, we selected for our numerical experiment a point within the heel of the curve. Therefore the parameters of the selected filters are as follows: radius of the inner transparent annulus $r_1 = 0.42$, radius of the outer annulus $r_2 = 0.96$. The light efficiency of the filter is $\eta = 0.25$. It is remarkable that the sidelobe height depends strongly on the value of ϵ. Therefore, if a different value for ϵ had been considered, different values for the proper radii of the annuli would have been obtained.

In Fig. 1 we have depicted with the solid curve the axial PSF of a 4Pi(C)-confocal microscope that incorporates the selected filter in the illumination set. Note, by comparing the curves in the figure, that the use of the proposed binary mask produces a severe reduction in the sidelobe strength. Specifically, the relative height of the lobe is ~5% of the main peak; i.e., a 75% sidelobe reduction is achieved. Let us emphasize that the obtained sidelobe height is approximately the same as the one obtained by use of two-photon excitation.[4] Of course, this low axial-sidelobe height permits the optimum use of nonlinear image-restoration techniques so that the axial resolution benefits fully from the approximately fourfold narrowness of the central peak of the axial PSF.

To make more complete the study of the influence of the proposed apodization technique on the performance of 4Pi-confocal microscopes, in Fig. 2 we show, with the solid curve, the so-called integrated intensity function (i.e., the z response to an infinitely thin fluorescent layer). Note that also in terms of this function of merit the use of the annular filters provides a noticeable improvement. In Fig. 7 we compare the transverse PSF of the apodized 4Pi-confocal microscope with the corresponding nonapodized counterpart, for the case of $\phi = \pi/2$. Note that only a slight widening is produced (~5% in terms of the FWHM), which does not compromise the lateral resolution of the system.

To finish, we center our attention on analyzing the form of the axial PSF of the illumination part of the 4Pi(C) microscope, which is given by the first factor in Eq. (2) provided that we consider the case $v = 0$. As is shown in Fig. 8, the use of the proposed annular filter with light efficiency $\eta = 0.25$ reduces the first axial-sidelobe strength, but it produces a severe enlargement of other secondary peaks. This can be important because, although this effect does not appear in the combined system PSF, it could result in severe photobleaching of the specimen at the position of the strong secondary peak. However, this effect can be overcome by using an annular filter of the same family but with higher efficiency. This is the case, shown in Fig. 8, of the filter with $\eta = 0.60$. Now the highest secondary lobe is slightly lower than the one obtained with the nonapodized 4Pi(C) setup. This improvement is obtained at the expense of a lower reduction of the sidelobe height of the combined system PSF. As can be inferred from Fig. 6, now the relative height of the axial sidelobe is ~12% of the main peak. This still represents a significant improvement in the axial contrast of the 4Pi(C) confocal microscope. We can conclude that proper selection of the binary filter should take into account two factors: the desired height of the sidelobe of the combined system PSF and the maximum permissible height of sidelobes of the illumination PSF. The compromise between the two factors determines the form of the adequate filter.

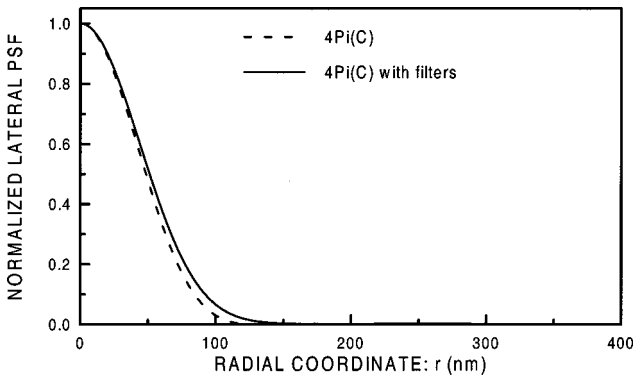

Fig. 7. Numerically evaluated transverse PSF for a 4Pi(C)-confocal microscope. For the calculation we considered $\phi = \pi/2$ in Eq. (2).

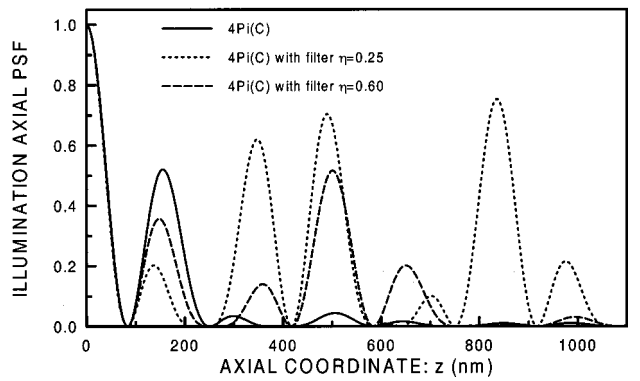

Fig. 8. Axial intensity PSF of the illumination part of a 4Pi(C)-confocal microscope.

Finally, we remark that the numerical experiments shown here were performed for the particular case of $\epsilon = 0.8$ and NA = 1.4. A change in the values of these parameters implies a modification of the height of the sidelobes (with or without pupil filters). But what it is clear is that by means of our design procedure, a proper pair of two-ring binary filters can be designed to achieve a significant reduction of the axial sidelobes.

5. CONCLUSIONS

We have presented a new technique for reduction of the sidelobe height of the axial PSF of one-photon 4Pi-confocal microscopes. The technique is based on the use of a pair of properly designed annular binary masks, and it allows the axial resolution to benefit fully from the narrowness of the central lobe of the axial PSF. The design procedure takes into account the following parameters: semiangular aperture of the lenses, α; refractive index n; wavelength ratio ϵ; maximum value allowable for the sidelobe height; and the requirement of minimizing the photobleaching effect. Specifically, we have obtained an axial PSF in which the height of the axial sidelobe is approximately 5% of the main peak. Further, we show that our method hardly affects the transverse resolution of the system.

Addendum: Sometime after the submission of this paper, a paper was published by other researchers[30] who had a similar idea but included the support of experimental results.

Part of this work was presented in the Focus on Microscopy 2001 Conference held in Amsterdam in April 2001. This research was funded by the Plan Nacional I + D + I (grant DPI2000-0774), Ministerio de Ciencia y Tecnología, Spain. We are indebted to the reviewers for their fine suggestions, which indeed improved the paper.

The corresponding author, Manuel Martínez-Corral, can be reached by phone, 34-9638-64343; fax, 34-9638-64715; or e-mail, manuel.martinez@uv.es. The e-mail address of Amparo Pons is Amparo.Pons-Marti@uv.es and of María-Teresa Caballero is mt.caballero@ua.es.

REFERENCES AND NOTES

1. M. Born and E. Wolf, *Principles of Optics* (Cambridge U. Press, Cambridge, UK, 1999), Chap. 8.
2. T. Wilson, ed., *Confocal Microscopy* (Academic, London, 1990).
3. S. Hell and E. H. K. Stelzer, "Properties of a 4Pi confocal fluorescence microscope," J. Opt. Soc. Am. A **9**, 2159–2166 (1992).
4. S. Hell and E. H. K. Stelzer, "Fundamental improvement of resolution with a 4Pi-confocal fluorescence microscope using two-photon excitation," Opt. Commun. **93**, 277–282 (1992).
5. S. W. Hell, S. Lindek, and E. H. K. Stelzer, "Enhancing the axial resolution in far-field light microscopy: two-photon 4Pi confocal fluorescence microscopy," J. Mod. Opt. **41**, 675–681 (1994).
6. M. Nagorni and S. W. Hell, "Coherent use of opposing lenses for axial resolution increase in fluorescence microscopy. I. Comparative study of concepts," J. Opt. Soc. Am. A **18**, 36–48 (2001).
7. P. E. Hänninen, S. W. Hell, J. Salo, and E. Soini, "Two-photon excitation 4Pi confocal microscope: enhanced resolution for biological research," Appl. Phys. Lett. **66**, 1698–1700 (1995).
8. M. Schrader, S. W. Hell, and H. T. M. van der Voort, "Three-dimensional super-resolution with 4Pi-confocal microscope using image restoration," J. Appl. Phys. **84**, 4033–4042 (1998).
9. M. Nagorni and S. W. Hell, "Coherent use of opposing lenses for axial resolution increase in fluorescence microscopy. II. Power and limitations of nonlinear image restoration," J. Opt. Soc. Am. A **18**, 49–51 (2001).
10. G. Toraldo di Francia, "Supergain antennas and optical resolving power," Nuovo Cimento Suppl. **9**, 426–435 (1952).
11. P. Jacquinot and B. Rozien-Dossier, "Apodization," in *Progress in Optics,* E. Wolf, ed. (North-Holland, Amsterdam, 1964), Vol. 3.
12. G. R. Boyer, "Réalisation d'un filtrage super-résolvant," Opt. Acta **30**, 807–816 (1983).
13. G. J. Brakenhoff, P. Blom, and P. Barends, "Confocal scanning light microscopy with high aperture immersion lenses," J. Microsc. **117**, 219–232 (1979).
14. Z. S. Hegedus and V. Sarafis, "Superresolving filters in confocally scanned imaging systems," J. Opt. Soc. Am. A **3**, 1892–1896 (1986).
15. S. W. Hell, P. E. Hänninen, A. Kuusisto, M. Schrader, and E. Soini, "Annular aperture two-photon excitation microscopy," Opt. Commun. **117**, 20–24 (1995).
16. M. Martínez-Corral, P. Andrés, J. Ojeda-Castañeda, and G. Saavedra, "Tunable axial superresolution by annular binary filters. Application to confocal microscopy," Opt. Commun. **119**, 491–498 (1995).
17. M. A. A. Neil, R. Juskaitis, T. Wilson, Z. J. Laczik, and V. Sarafis, "Optimized pupil-plane filters for confocal microscope point-spread function engineering," Opt. Lett. **25**, 245–247 (2000).
18. M. Martínez-Corral, P. Andrés, C. J. Zapata-Rodríguez, and C. J. R. Sheppard, "Improvement of three-dimensional resolution in confocal scanning microscopy by combination of two pupil filters," Optik (Stuttgart) **107**, 145–148 (1998).
19. Z. Ding, G. Wang, M. Gu, Z. Wang, and Z. Fan, "Superresolution with an apodization film in a confocal setup," Appl. Opt. **36**, 360–363 (1997).
20. M. Kowalczyk, C. J. Zapata-Rodríguez, and M. Martínez-Corral, "Asymmetric apodization in confocal imaging systems," Appl. Opt. **37**, 8206–8214 (1998).
21. M. Martínez-Corral, P. Andrés, C. J. Zapata-Rodríguez, and M. Kowalczyk, "Three-dimensional superresolution by annular binary filters," Opt. Commun. **165**, 267–278 (1999).
22. C. J. R. Sheppard, "Binary optics and confocal imaging," Opt. Lett. **24**, 505–506 (1999).
23. S. W. Hell, S. Lindek, C. Cremer, and E. H. K. Stelzer, "Measurement of the 4Pi-confocal point spread function proves 75 nm axial resolution," Appl. Phys. Lett. **64**, 1335–1337 (1994).
24. The term apodization etymologically comes from the Greek (to remove foot), and involves the suppression, or at least a considerable decrease, of the sidelobes of the PSF.
25. B. Richards and E. Wolf, "Electromagnetic diffraction in optical systems. II. Structure of the image field in an aplanatic system," Proc. R. Soc. London Ser. A **253**, 358–379 (1959).
26. M. Gu, *Advanced Optical Imaging Theory* (Springer-Verlag, Berlin, 2000).
27. C. J. R. Sheppard and H. J. Matthews, "Imaging in high-aperture optical systems," J. Opt. Soc. Am. A **4**, 1354–1360 (1987).
28. C. W. McCutchen, "Generalized aperture and the three-dimensional diffraction image," J. Opt. Soc. Am. **54**, 240–244 (1964).
29. S. Grill and E. H. K. Stelzer, "Method to calculate lateral and axial gain factors of optical setups with a large solid angle," J. Opt. Soc. Am. A **16**, 2658–2665 (1999).
30. C. M. Blanca, J. Bewersdorf, and S. W. Hell, "Single sharp spot in fluorescence microscopy of two opposing lenses," Appl. Phys. Lett. **79**, 2321–2323 (2001).